

## Recalibration of the Soft X-ray Telescope on *Yohkoh*

Loren W. Acton

© Springer ●●●

**Abstract** This paper presents a new derivation of the x-ray sensitivity of the Soft X-ray Telescope (SXT) experiment on *Yohkoh*. The recalibration is based upon the hypothesis that, during the first 15 months of the mission, an absorbing material gradually built up on the entrance filters of the telescope. I have also re-evaluated the times and sizes of ruptures of the SXT entrance filters. The impact of this recalibration on derived filter-ratio temperature, emission measure and calculated spectral irradiance is substantial, especially prior to 1992 November. X-ray fluxes at earth are presented, based upon this recalibration.

**Keywords:** Sun, Corona, Instrumental effects, Data calibration

### 1. Introduction

The Soft X-ray Telescope (SXT) experiment on the Japan/US/UK *Yohkoh* mission recorded x-ray images of the full-sun, active regions, and flares in the (nominal) 0.3-3.0 nm band for the period 1991 October to 2001 December 14. The *Yohkoh* mission is described in the collection of articles edited by Švestka and Uchida (1991). The individual papers are also available on the *Yohkoh* Legacy Archive (YLA) website (Takeda *et al.*, 2009; Takeda, 2015; Acton, 2017). The solar observations by *Yohkoh* are archived in their entirety in the YLA (<http://solar.physics.montana.edu/ylegacy/>) and at ISAS/JAXA in Japan (<http://darts.isas.jaxa.jp/solar/yohkoh/>) as well as the Solar Data Analysis Center of NASA Goddard Space Flight Center ([http://umbra.nascom.nasa.gov/yohkoh/y4sdac\\_top.html](http://umbra.nascom.nasa.gov/yohkoh/y4sdac_top.html)). The latter archives provide less reduced data and related information than the YLA.

The SXT instrument has been described by Tsuneta *et al.* (1991). On-orbit data issues and calibration are exhaustively treated by Acton (2016). There it is explained that the entrance apertures of the SXT were covered by duplex entrance filters. The individual filters are mounted on frames each of which covers

---

✉ L. W. Acton  
e-mail: [loren.acton@montana.edu](mailto:loren.acton@montana.edu)

Department of Physics, Montana State University, P.O. Box 173840, Bozeman, MT 59717-3840 USA

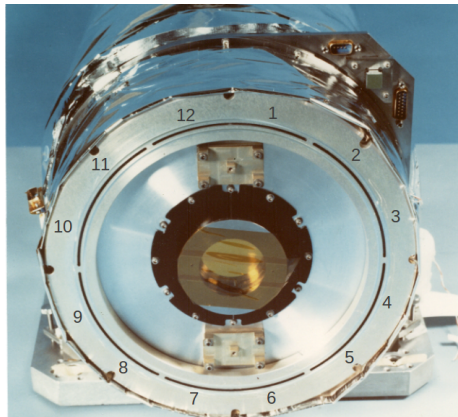


**Figure 1.** SXT entrance apertures with filter sectors numbered.

a 60 degree sector of the entrance annulus. Each frame comprises two individual 30 degree sections for a total of 12 sectors. The filter membrane is Lexan plastic 180 nm thick covered with 70 nm of Ti (to exclude He II, 30.4 nm) and 90 nm of Al for thermal control and to exclude visible light. For the outer ring of filters the Al layer faces the sun. The x-ray entrance filters encircle the visible-light aspect telescope as shown in Figure 1.

In the course of this re-examination of SXT calibration I have concluded that some absorbing material was deposited on the SXT aspect telescope entrance window and the outer x-ray entrance filters during the first  $\sim 15$  months of the mission. For want of better knowledge I assume that this material is carbon (C), reaching a total thickness of about  $0.225 \mu\text{m}$  by the time (1992 November) that additional deposition became inconsequential. I have also re-examined the timing and magnitude of each entrance filter failure. The analysis details for this recalibration are given in the following sections.

The deposition of absorbing material (hereafter referred to simply as C, for carbon) and opening up of each entrance filter sector changed the spectral sensitivity of the SXT. Thus, derivation of, e.g., temperature and emission measure from filter ratios must take these changes into account. The changes in SXT sensitivity were only approximately accounted for in previous calibrations (Acton, 2016). They are fully treated in the results presented in this paper and in the updated SXT data analysis software archived in SolarSoft (<https://sohowww.nascom.nasa.gov/solarsoft/>).

## 2. The Case for Entrance Filter Contamination

All elements of the SXT optical train were calibrated in the laboratory. End-to-end testing of the SXT under vacuum was consistent with the piecewise calibration results. *SXT Calibration Notes 5* (Lemen and Hudson, 1990), *29* (Acton, 1992), and *30* (Lemen, 1992), which are available in the YLA, detail aspects of pre-launch calibration and testing. On-orbit issues affecting SXT calibration have been discussed by Acton (2016).

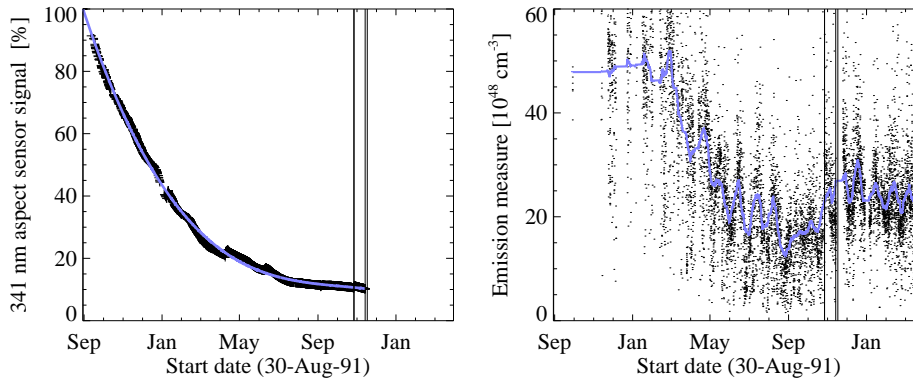


**Figure 2.** Left: Decay of aspect sensor signal, overlaid (blue line) with a third-order polynomial fit to the data. This curve is used to calculate the build up of C on the x-ray entrance filters. Right: Full-sun emission measure derived from 9510 filter-ratio pairs acquired prior to 1993 April 1. The blue line is a 301 point boxcar smoothing of the emission measure results. Twenty seven day modulation of the emission measures, from solar rotation, is evident. The vertical lines in both panels denote times of entrance filter ruptures.

Although the signal from the SXT aspect telescope (usually referred to as the SXT aspect sensor) at 341 nm decreased exponentially immediately after launch (Figure 2), and had reached a level of about 8% by 1992 November. The physical reason for the decay remained a mystery for more than 3 decades. Deposition of some absorbing material on the entrance optic of the aspect sensor was rejected as the cause for two reasons. (1) The black Chemglaze paint on the inner side the aluminum closeout plate immediately in front of the SXT had been chosen as an acceptable low-outgas material and had been prepared and baked out according to NASA-approved methods and no other probable source of contaminating material was identified. (2) X-ray images from the SXT revealed no obvious signature concurrent with the signal decline of the aspect sensor.

Recently, in the course of deriving soft x-ray irradiance for the entire *Yohkoh* mission, I noticed the strange time evolution of derived emission measure depicted in Figure 2. The steep fall-off emission measure and its sharp increase across the times of the first entrance filter failures suggest that the calibration prior to those ruptures employed an SXT effective area greater than was actually the case. This result would be experienced if some absorbing material accumulated on all front-end x-ray apertures in parallel with the contamination of the aspect sensor entrance window. In such a scenario the amount of contaminant must be substantial to absorb 90 percent of the 341 nm light falling on the aspect sensor outer window. Think of how dirty your spectacles would need to be to cause the loss of 90 percent of the light entering your eye. Such a layer of absorbing material accumulating on the x-ray entrance filters, covering the Al outer layer, would also severely change the thermal properties of these thin membranes, producing an enhanced thermal shock at every sunrise. (Note that, as far as we can tell, all entrance filter failures took place at orbital sunrise.) Failure to take into account the diminishing sensitivity of the SXT as the contaminant built up

**Table 1.** X-ray Transmission of an Entrance Filter Sector versus Wavelength.

Wavelength (nm)	Launch	Launch	1992 Oct	1992 Oct	No filt
	Both filts	Inner only	Both filts	Inner only	
0.50	0.89	0.95	0.89	0.95	1.00
1.00	0.73	0.85	0.69	0.85	1.00
1.50	0.41	0.64	0.34	0.64	1.00
2.00	0.17	0.41	0.11	0.41	1.00

would produce the time profile of emission measure shown in Figure 2. Looking ahead at results of this recalibration, values of SXT entrance filter transmission, caused by deposition of C and failure of an outer entrance filter, are given in Table 1

### 3. SXT Recalibration

We have no knowledge of what material accumulated on the SXT entrance apertures but, whatever it is, it is likely to include C in its composition. Unfortunately, the aspect sensor decay curve, while it provides the fractional rate of C deposition, does not itself yield the thickness of the hypothesized C layer. The linear absorption coefficient of C at 341 nm ( $C_{\text{sigma}}$ ) appears to depend strongly upon deposition conditions and ranges from 0.75 (Dasgupta *et al.*, 1991) to 2.3 (Palik, 1991) to 13 (Laidani *et al.*, 2008)  $\mu\text{m}^{-1}$  in the literature. On the other hand, the absorption coefficient of C in x-rays is well determined so I will turn to the x-ray image data to learn the thickness of a C layer.

The outer entrance filter failures of 1992 October 27, one orbit apart at 05:41 and 07:18, provide the best opportunity to determine the effective thickness of the C layer at the time that entrance filters began to fail. This was a period of high flare activity but we were fortunate to obtain thin-Al and Al/Mn/Mg filter pairs (see (Acton, 2016) for descriptions of the SXT analysis filters) with comparable GOES flux levels before and after the 2 failures as illustrated in Figure 3.

In order to avoid, as much as possible, variations in coronal x-ray signal over this interval the region around the south pole as delineated by Figure 3 was selected for analysis. It is convenient to parameterize the analysis of the C layer in terms of the (unknown) linear absorption coefficient ( $C_{\text{sigma}}$ ) at 341 nm, the wavelength of the narrow-band aspect sensor images. This readily converts to C thickness.

A perfect match across the filter failures requires  $C_{\text{sigma}}=9.6$  for temperature and  $C_{\text{sigma}}=10.7$  for emission measure. Thus, we have chosen  $C_{\text{sigma}}=10.1$ , corresponding to a C thickness of  $0.225 \mu\text{m}$ . It is encouraging that the derived value of  $C_{\text{sigma}}$  (i.e., 10.1) falls within the published range mentioned above. Figure 4 demonstrates the result of the SXT entrance filter recalibration including the C layer. A satisfactory match is achieved for both temperature and emission measure.

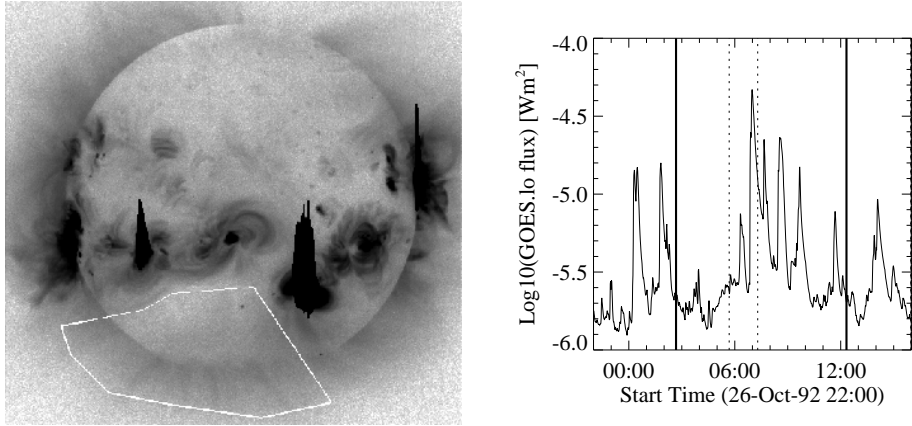


**Figure 3.** Left: SXT Al.1 image of 27-Oct-92 12:19:37. South polar region used for Csigma analysis indicated by the white line. Right: Times of SXT image pairs used for C thickness analysis compared to GOES low channel 1-8 Å flux. Vertical broken lines denote times of outer entrance filter failures. Heavy vertical lines mark times of SXT image pairs.

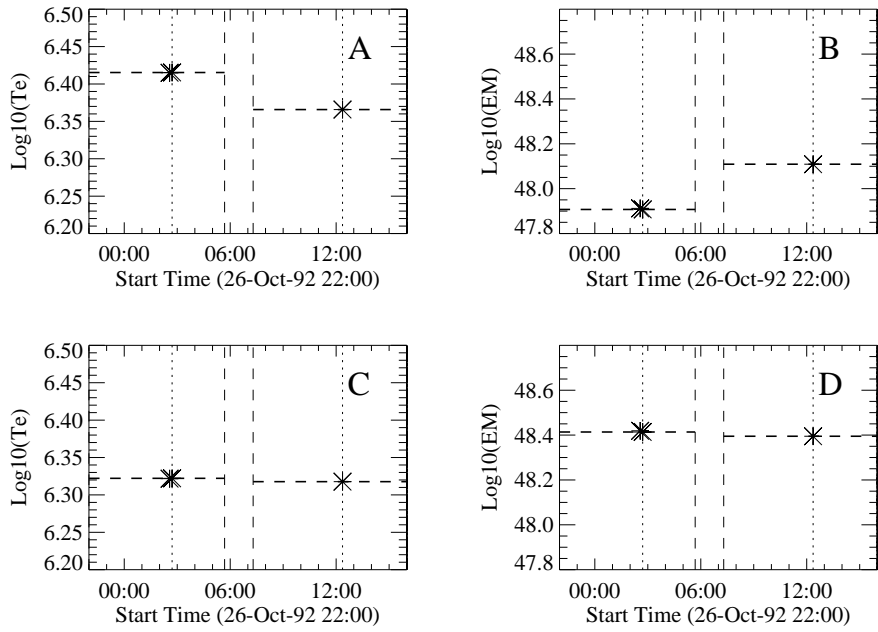


**Figure 4.** Panels A and B show the mismatch of coronal temperature and emission measure across the entrance failures for the launch calibration. Panels C and D are the corresponding transitions for a carbon deposition layer of 0.225  $\mu\text{m}$ .

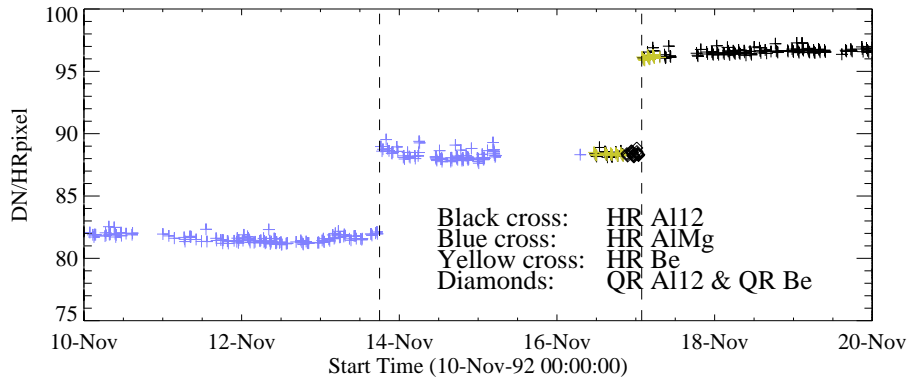


**Figure 5.** Signals from a small area in the lower right corner of raw x-ray images for various resolution and analysis filters. The units given on the Y-axis refer to the blue crosses. Other data have been adjusted to the half-resolution (HR) data taken through the AlMg filter. The steps are caused by increases in visible straylight reaching the focal plane at the times of entrance filter ruptures.

**Table 2.** Revised Sequence of SXT Entrance Filter Failures

Date (nm)	Outer Sectors	Inner Sectors
30-Aug-91 10:30	0.0	0.0
27-Oct-92 05:41	1.0	0.0
27-Oct-92 07:18	2.0	0.0
13-Nov-92 18:00	2.0	1.0
17-Nov-92 01:47	2.0	2.0
16-Aug-95 08:04	4.0	4.0
24-Aug-96 07:00	5.0	5.0
24-Jan-98 00:00	6.0	6.0
30-Jan-99 23:17	8.0	7.0
12-Mar-99 02:00	8.0	7.5
20-Apr-99 19:02	8.0	8.0
14-Dec-01 21:12	8.0	8.0

Acton (2016) discusses, in detail, the sequence of failures of the SXT entrance filter based primarily upon visible straylight within the telescope. In this work straylight signatures in the corners, with little or no x-ray illumination, of the raw full-frame x-ray images have been included in the analysis. It was thus discovered that the double 1992 November inner-filter ruptures took place in two steps as shown in Figure 5. All failure events were examined in a similar manner. Table 2 presents the conclusions of this work. Note that, after 1992 October, it is not possible to see straylight effects from ruptures in outer entrance filters alone so the table gives the same values for the number of open sectors for both outer and inner filters.

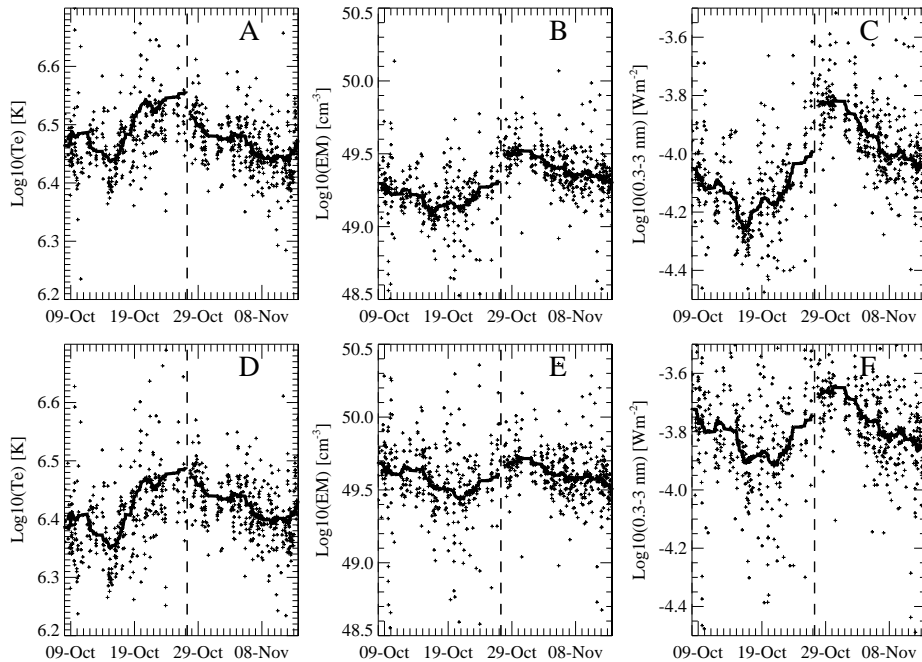


**Figure 6.** Panels A, B, and C show the mismatch of the run of derived full-sun coronal temperature, emission measure, and 0.3-3 nm irradiance across the first two entrance failures for the old calibration. Panels D, E, and F illustrate the improvement with the new SXT calibration with a carbon deposition layer reaching  $0.225 \mu\text{m}$  in thickness. The solid lines are generated with a 61-datum running boxcar smoothing.

#### 4. Results of the Recalibration

Figure 6 illustrates the improved match of physical parameters derived from SXT full-sun filter pairs across the time of the two outer-filter ruptures of 1992 October 27. Note that coronal temperatures are decreased and emission measures and derived fluxes are increased by the new calibration.

The primary physical parameter derived from SXT filter pairs is the temperature. Emission measure ( $\int N_e^2 dV$ ) is derived from temperature and the signal in either of the filters and irradiance in a spectral band is calculated from temperature, emission measure, and a spectral model from Chianti version 8.0 (Dere *et al.*, 1997; Landi *et al.*, 2013; Del Zanna *et al.*, 2015) using `sun_coronal_2012_schmelz.abund` and `chianti.ioneq`. Figure 7 presents the logarithms of full-sun temperature and 0.3-3 nm irradiance for the entire mission. Note the greater scatter in the results for the period prior to the first entrance filter ruptures in 1992 October. There are two reasons for this. (1) Techniques for dark frame acquisition and subtraction reached maturity around this time and (2) with the added C layer on the entrance filters the slope of the Te versus filter-ratio calibration curve became steeper, making Te determinations more sensitive to the precise value of the filter ratio.

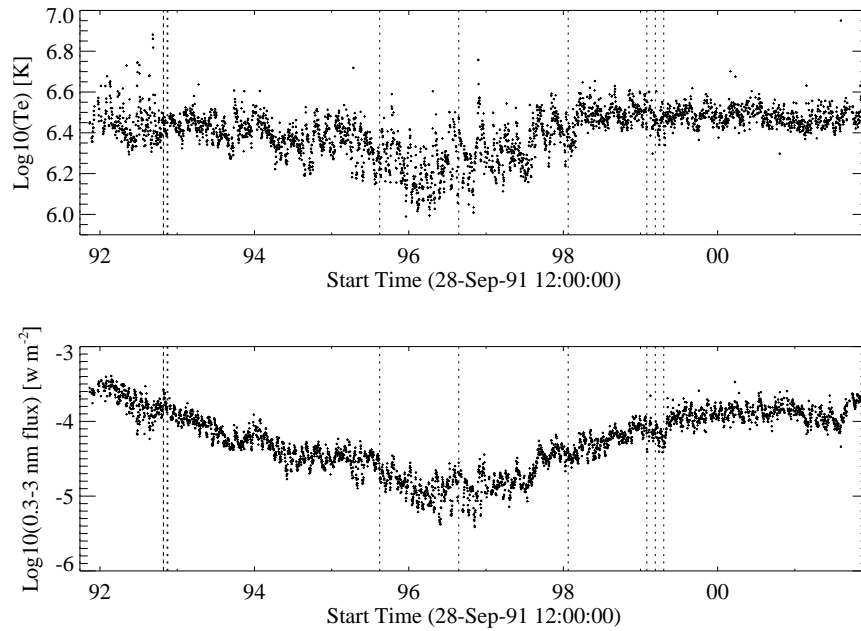


**Figure 7.** Top: Daily average full-sun coronal temperature derived from 65,282 SXT filter pairs, using the new calibration reported herein. Vertical dotted lines denote times of entrance filter failures. Bottom: Corresponding irradiance at earth in the 0.3-3 nm band from SXT observations.

## 5. Conclusion

I conclude that the analysis of SXT data reported here support the hypothesis that some carbon-like material deposited on the entrance apertures of the SXT. The rate of deposition decreased to near zero by the end of 1992 and its impact on calibration became of less importance as sectors of the entrance filters rupyutr as listed in Table 2 and illustrated in Figure 8.

As demonstrated in Figure 8, published SXT analyses using the old calibration for post-1992-November SXT observations should not be seriously impacted by this recalibration.

**Acknowledgments** I sincerely thank the Physics Department of Montana State University for an Emeritus position and the use of the infrastructure necessary to do this research. Dr. Aki Takeda, creator of the YLA, has contributed to this work in many ways. This paper capitalizes on the *Yohkoh* mission, software and data products supported by NASA over several decades.

## References

- Acton, L.: 1992, *SXT Calibration Note 29. Preliminary Calibration of SXT Flight X-ray Filters*. [http://solar.physics.montana.edu/ylegacy/documents/sxt\\_cal\\_note/SXT\\_cal\\_note\\_29.pdf](http://solar.physics.montana.edu/ylegacy/documents/sxt_cal_note/SXT_cal_note_29.pdf).

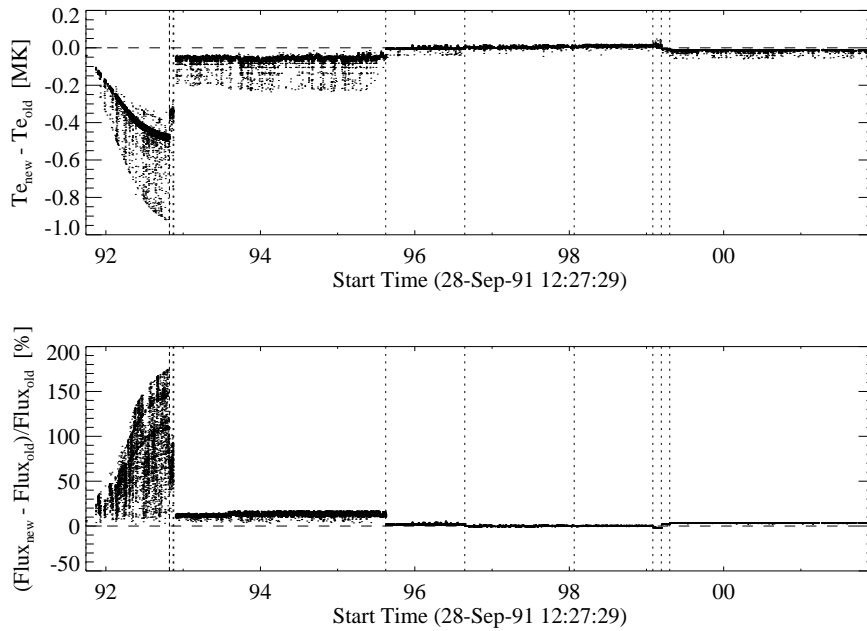


**Figure 8.** Top: Difference in derived coronal temperature resulting from the new SXT calibration. Bottom: Percent difference in 0.3-3 nm irradiance resulting from use of the new calibration.

- Acton, L.W.: 2016, On-Orbit Performance and Calibration of the Soft X-Ray Telescope on Yohkoh. *Solar Phys.* **291**, 643. DOI. ADS.
- Acton, L.W.: 2017, The Yohkoh Legacy (Data) Archive. *Phys. & Astron. Int'l Journal* **1**(3), 00019. DOI.
- Dasgupta, D., Demichelis, F., Pirri, C.F., Tagliaferro, A.: 1991,  $\pi$  bands and gap states from optical absorption and electron-spin-resonance studies on amorphous carbon and amorphous hydrogenated carbon films. *Phys. Review B* **43**, 2131. DOI. ADS.
- Del Zanna, G., Dere, K.P., Young, P.R., Landi, E., Mason, H.E.: 2015, CHIANTI - An atomic database for emission lines. Version 8. *Astron. Astrophys.* **582**, A56. DOI. ADS.
- Dere, K.P., Landi, E., Mason, H.E., Monsignori Fossi, B.C., Young, P.R.: 1997, CHIANTI - an atomic database for emission lines. *Astron. Astrophys. Suppl.* **125**, 149. DOI. ADS.
- Laidani, N., Bartali, R., Gottardi, G., Anderle, M., Cheyssac, P.: 2008, Optical absorption parameters of amorphous carbon films from Forouhi Bloomer and Tauc Lorentz models: a comparative study. *Journal of Physics Condensed Matter* **20**(1), 015216. DOI. ADS.
- Landi, E., Young, P.R., Dere, K.P., Del Zanna, G., Mason, H.E.: 2013, CHIANTI Atomic Database for Emission Lines. XIII. Soft X-Ray Improvements and Other Changes. *Astrophys. J.* **763**, 86. DOI. ADS.
- Lemen, J.R.: 1992, *SXT Calibration Note 30. Effective Area of SXT Mirror (In-Flight)*. [http://solar.physics.montana.edu/ylegacy/documents/sxt.cal.note/SXT\\_cal.note.30.pdf](http://solar.physics.montana.edu/ylegacy/documents/sxt.cal.note/SXT_cal.note.30.pdf).
- Lemen, J.R., Hudson, H.S.: 1990, *SXT Calibration Note 5. The SXT X-ray Neutral-density Filters*. [http://solar.physics.montana.edu/ylegacy/documents/sxt.cal.note/SXT\\_cal.note.5.pdf](http://solar.physics.montana.edu/ylegacy/documents/sxt.cal.note/SXT_cal.note.5.pdf).
- Palik, E.D.: 1991, *Handbook of optical constants of solids II*. ADS.
- Švestka, Z., Uchida, U. (eds.): 1991, *The YOHKOH (SOLAR-A) Mission*, Kluwer, Dordrecht.
- Takeda, A.: 2015, *Yohkoh Legacy Data Archive*. <http://solar.physics.montana.edu/ylegacy>.
- Takeda, A., Acton, L., McKenzie, D., Yoshimura, K., Freeland, S.: 2009, Resident archive services of the yohkoh legacy data archive. *Data Sci. J.* **8**, IGY1. DOI.

Tsuneta, S., Acton, L., Bruner, M., Lemen, J., Brown, W., Carvalho, R., Catura, R., Freeland, S., Jurcevich, B., Owens, J.: 1991, The Soft X-ray Telescope for the SOLAR-A mission. *Solar Phys.* **136**, 37. DOI. ADS.